Analysis of the Effects of Soil Thermal Properties on the Performance of an Earth-Air Heat Exchanger

Gustavo Chaves Carraro, Carlos Henrique Diedrich, Gerson Henrique dos Santos *, Victor Vaurek Dimbarre and Thiago Antonini Alves

Graduate Program in Mechanical Engineering (PPGEM), Federal University of Technology - Parana (UTFPR), Rua Doutor Washington Subtil Chueire, 330, Ponta Grossa, 84017-220, PR, Brazil;
**Correspondence:gsantos@utfpr.edu.br*

Abstract. Among the ways to obtain good thermo-energetic performance in buildings, passive air conditioning stands out. These systems use the potential of the local climate and the characteristics of the building envelope to promote thermal comfort for the occupants, using low energy costs, as is the case with Earth-Air Heat Exchangers (EAHE). In this system, ambient air circulates through a pipe buried at a certain depth in the ground, causing it to heat up or cool down, depending on weather conditions. These effects are possible due to the high thermal inertia that keeps the soil at an almost constant temperature, at specific depths, even with high external temperature amplitudes. In this context, the performance of EAHE depends directly on the thermal properties of the soil. Thus, numerical simulations will be performed using the Ansys/Fluent software. The effects of the thermal properties of different types of soils will be verified on the thermal performance of these exchangers. An EAHE prototype was installed at the Federal University of Technology – Paraná (UTFPR) to validate the numerical model.

Keywords: earth-air heat exchanger, thermal properties of soils, computational fluid dynamics

1 Introduction

According to the International Energy Association [1], using air conditioning systems for environmental conditioning accounts for nearly 20% of the electricity consumed in buildings around the world, and this trend is expected to increase as economic development and population growth reaches hotter climate countries. Out of the 2.8 billion people living in the hottest regions of the world, only 8% have air conditioning, while in the United States, for example, 90% of households are equipped with such devices. Energy consumption for climate control grew faster than for any other purpose between 1990 and 2016, more than tripling. In the search for more sustainable methods of climate control, Earth-Air Heat Exchangers (EAHE) are alternatives that offer much lower energy consumption, as these systems take advantage of the thermal inertia of the ground to heat or cool the air that circulates through them, using electricity only to facilitate the air circulation within the system.

Several studies on EAHE can be found in the literature. Khabbaz et al. [2] conducted a study analyzing an EAHE's performance in Marrakesh, comparing the experimental results to those obtained through a numerical model. It was shown that even in the hottest hour of a summer day when the inlet temperature was above 308 K, the EAHE could cool down the air to an outlet temperature of approximately 295 K. Brum [3] developed a simplified numerical model of an EAHE and also simulated the behavior of soil temperature at different depths throughout the year, then compared the results obtained with the numerical solution to the experimental data to validate the model. It was shown that at a depth of 2 m, for example, the EAHE can cool the air by more than 7K in a hot month and can warm up the air by almost 3 K during a cold month. D'Agostino et al. [4] also developed a numerical model of an EAHE and compared its performance in the soils and climates of different cities worldwide, demonstrating that these parameters significantly impact the performance of the EAHE. Misra et al. [5] used a numerical model of an EAHE to evaluate the performance deterioration under transient conditions, comparing the effects of different soil thermal conductivities, air inlet velocities, and pipe diameters.

Based on the validation of the numerical model of the EAHE built at the Federal University of Technology—Parana, Ponta Grossa/Brazil (25.1° South, 50.16° West) through comparison with experimental data, as shown in the work of Diedrich et al. [6], this study aims to expand the scope of research by investigating, using the computational model, the behavior of the EAHE in different types of soils under both dry and saturated conditions. This research builds upon studies in the field of soil type influence and saturation on their thermal properties, evaluating how the performance of the EAHE is affected by these distinct conditions in both summer and winter.

2 Methodology

The methodology employed for the numerical study presented in this work is based on the use of Computational Fluid Dynamics (CFD) to solve the Reynolds-Averaged Navier-Stokes equations (URANS), utilizing the ANSYS/Fluent® 2021 R1 software for this purpose. To predict the thermal behavior of the soil throughout the year at various depths, the model proposed by Kusuda and Archenbach [7] has been utilized.

2.1 Mathematical Model

According to the model presented in Tannehill [8], the *continuity equation* for a incompressible fluid is expressed by eq. (1).

$$\nabla . \vec{v} = 0 \tag{1}$$

In the eq. (1), $\vec{v}$ is the velocity vector of the fluid and ∇ is the divergent differential operator. Considering that no external forces act on the diferencial mass element, the convervation equation of momentum takes the form shown in eq. (2).

$$\rho \frac{D\vec{v}}{Dt} = \nabla p + \rho \vec{g} + \mu \nabla^2 \vec{v} \tag{2}$$

In eq. (2), in addition to the terms seen in eq. (1), ρ is the fluid density, $\vec{g}$ is the gravitational acceleration, μ is dynamic viscosity, and p is static pressure.

The energy equation in the studied model is shown in eq. (3).

$$\rho \frac{De}{Dt} = \frac{\partial Q}{\partial t} + k \nabla^2 T + \varphi \tag{3}$$

The new terms in eq. (3) are the energy by unit mass e, the heat transferred by unit volume Q, the thermal conductivity k, the temperature T and the rate of energy dissipation φ.

The turbulence model utilized was the $k - \varepsilon$ *Standard*. The transport equations of this model are the eq. (4) and eq. (5).

$$\frac{\partial}{\partial t}(\rho k) + \frac{\partial}{\partial x_j}(\rho k u_j) = \frac{\partial}{\partial x_j}\left[\left(\mu + \frac{\mu_t}{\sigma_k}\right)\frac{\partial k}{\partial x_j}\right] + G_k + G_b - \rho\epsilon \tag{4}$$

$$\frac{\partial}{\partial t}(\rho \epsilon) + \frac{\partial}{\partial x_j}(\rho \epsilon u_j) = \frac{\partial}{\partial x_j}\left[\left(\mu + \frac{\mu_t}{\sigma_\epsilon}\right)\frac{\partial \epsilon}{\partial x_j}\right] + C_{1\epsilon}\frac{\epsilon}{k}(G_k - C_{3\epsilon}G_b) - C_{2\epsilon}\rho\frac{\epsilon^2}{k} \tag{5}$$

In eq. (4) and eq. (5), ϵ, represents the rate of turbulent energy dissipation, σ_k and σ_ϵ are the turbulent Prandtl numbers for k and ϵ, respectively, G_k is the generation of turbulent kinetic energy due to average velocity gradients, G_b It's the generation of turbulent kinetic energy due to buoyancy, and μ_t is the turbulent viscosity, which can be calculated using eq. (6).

$$\mu_t = \rho C_\mu \frac{k^2}{\epsilon} \tag{6}$$

The constants shown in eq. (4) and eq. (5) were chosen according to their default values assigned by Fluent®, which are listed in Tab. 1.

Table 1. Constants utilized in the turbulence model

$C_{1\epsilon}$	$C_{2\epsilon}$	$C_{3\epsilon}$	C_{μ}	σ_k	σ_ϵ
1.44	1.92	-0.33	0.09	1	1.3

The solution method adopted in ANSYS/Fluent® for the coupling of pressure and velocity was the SIMPLE method, with a first-order upwind scheme for turbulent kinetic energy and its dissipation, and a second-order upwind scheme for the conservation equations of momentum and energy. In the solution controls, the relaxation factors used were 0.3 for pressure, 1 for density, 1 for body forces, 0.7 for momentum, 0.8 for turbulent kinetic energy, 0.8 for turbulent dissipation rate, 1 for turbulent viscosity, and 1 for energy.

2.2 Geometry and Mesh generation

The geometry of the EAHE was reproduced using ANSYS® Design Modeler, following the dimensions of the prototype built at UTFPR – Ponta Grossa (shown in Fig. 1), as presented in Diedrich [9]. The dimensions of the EAHE and the soil domain are shown in Tab. 2 and Tab. 3, respectively, resulting in the geometry displayed in Fig. 2. To optimize the numerical analysis of EAHE, a reduced soil domain extending 0.5 m in all directions from the heat exchanger serpentine was considered. As boundary conditions, constant temperatures were imposed on the upper and lower surfaces of the soil domain, while the other surfaces were considered adiabatic.

Table 2. Dimensions of the EAHE

N. of steps	Distance between the pipes (m)	Depth (m)	External Diameter (m)	Total length (m)
8	0.5	1.5	0.1	48.2

Table 3. Dimensions of the soil domain in the simulations

Length (m)	Width (m)	Height (m)
6.7	4.75	1

Figure 1. The experimental model of the EAHE built at UTFPR – Ponta Grossa

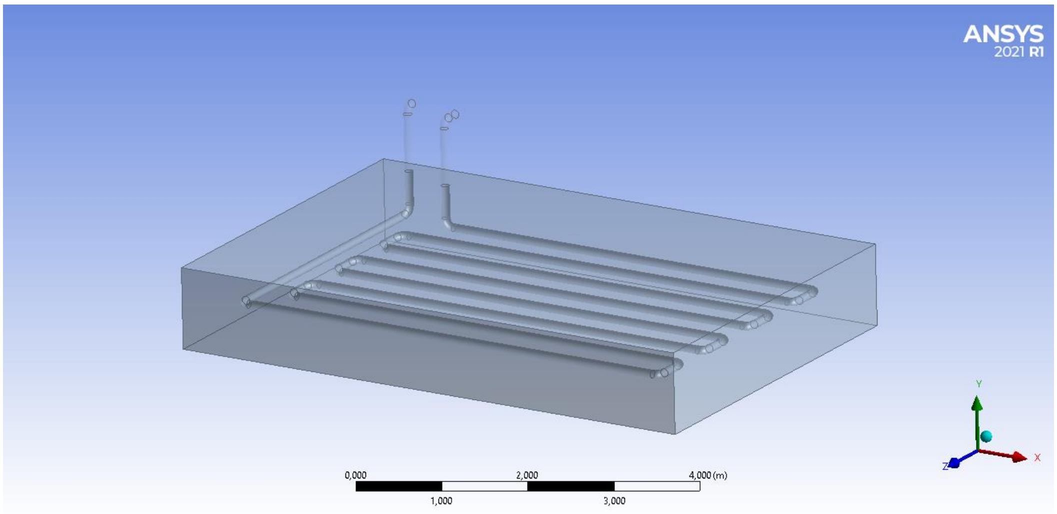

Figure 2. Geometry created using ANSYS® *Design Modeler*.

After creating the geometry, the mesh was generated, as shown in Fig. 3. The mesh refinement option Edge Sizing was used, and the "capture curvature and proximity" option was enabled to adapt the mesh to the geometry. The generated mesh consisted of 3,683,460 elements. Using the Orthogonal Quality metric, it was observed that the element with the lowest quality was 0.15799, following the good practice of aiming to keep it above 0.1.

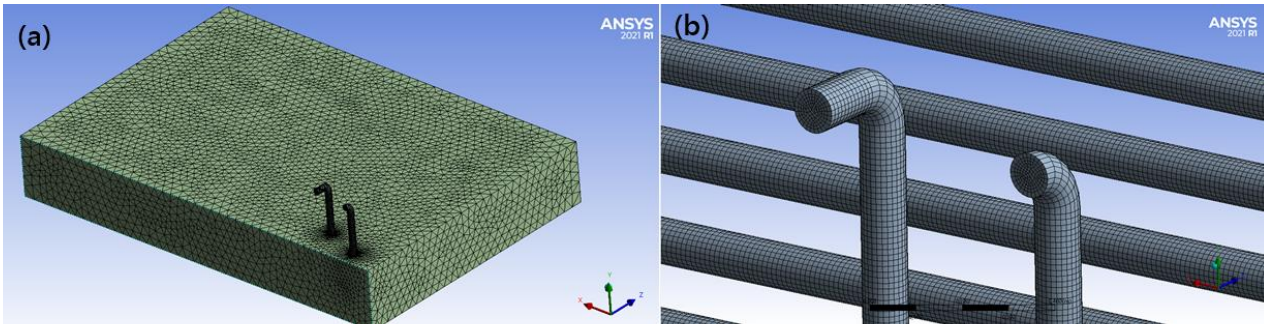

Figure 3. (a): Mesh of both soil and air domains. (b): Mesh of air domain only.

2.3 Simulation Procedures

The inlet velocity of the air was set at 0.774 m/s based on experimental data. The side walls of the soil domain were considered adiabatic. For the EAHE outlet, a condition of zero gauge pressure was used.

The inlet temperature was modeled through the User Defined Functions (UDFs). The polynomial curve fittings were generated using experimental data related to inlet temperatures during a summer day (01/23/2022) and a winter day (08/20/2022). In both cases, two polynomials were generated to achieve more precision.

Regarding the upper and bottom walls, the fixed temperature boundary condition was used based on the average temperatures of the analyzed soils at 1m and 2m depth, respectively, on 01/23/2022 (summer) and 08/20/2022 (winter). These temperatures were obtained through the model proposed by Kusuda and Archenbach [7]. This model is also used in other works in the field, such as the one by D'Agostino et al. [4] and Brum [3], and it is based on the theory of the semi-infinite solid, as seen in eq. (7).

$$T_{soil}(z,t) = \bar{T}_{surf} + a_{surf}.\, e^{-z.\sqrt{\frac{\pi}{365.\alpha}}}.\, cos\left(\frac{2\pi}{365}(t - t_{max}) - \frac{z}{2}\sqrt{\frac{365}{\pi.\alpha}}\right) \tag{7}$$

In eq. (7), z is the depth, t is the time (in days), $\bar{T}_{surf}$ is the average ground temperature, t_{max} is the day of the year in which the highest temperature was reached, a_{surf} is the amplitude of the variation in ground surface temperature and α is the termal diffusivity. The properties of each soil analyzed and the parameters used in eq. (7) are shown in Tab. 4 and Tab. 5, respectively.

Table 4. Properties of the soils analyzed (Hamdhan and Clarke [10])

	Sand(dry)	Sand(saturated)	Clay(dry)	Clay(saturated)
$k(W/(m.K))$	0.27	3.34	0.25	1.52
$\rho(kg/m^3)$	1700	2080	1390	1730
$C_p(J/(kg.K))$	800	1483	800	2362
$\alpha(m^2/day)$	0.01715	0.09355	0.01942	0.03213

Table 5. Parameters used in eq. (7) (Mendes et al. [11])

$\bar{T}_{surf}(K)$	$a_{surf}(K)$	$t_{max}(day)$
293.6	280.28	11

The temperatures used as boundary conditions in the upper and bottom walls of the soil domain were finally set for each simulation, as indicated in Tab. 6.

Table 6. Temperatures of each soil analyzed at 1m and 2m depth at 01/23/2022 and 08/20/2022.

Soil	Depth (m)	01/23/2022 Temperatures	08/20/2022 Temperatures
Sand(dry)	1	296.6 K	290.4 K
	2	294.2 K	291.9 K
Sand(saturated)	1	298.8 K	290.0 K
	2	297.2 K	290.2 K
Clay(dry)	1	296.9 K	289.9 K
	2	294.4 K	291.8 K
Clay(saturated)	1	297.6 K	290.1 K
	2	295.3 K	291.1 K

3 Results

Figure 4 shows the average ground temperatures at depths of 1m and 2m throughout the year, while Fig. 5 and Fig. 6 display the temperature profiles obtained from the simulations. Figure 5 illustrates the average temperature profile through the EAHE during the summer day (01/23/2022), where the Heat Exchanger is expected to cool the air, which has a higher temperature compared to the ground. Meanwhile, Fig. 6 demonstrates the winter case (08/20/2022), in which the EAHE is expected to warm the air, as the inlet temperatures are colder than the ground. Each simulation required a computational time of 25 minutes on a computer equipped with the NVIDIA® GeForce GTX 1660 Super 6GB GDDR6 graphics card, 16GB DDR5 RAM, and an Intel® Core i5-10400f processor.

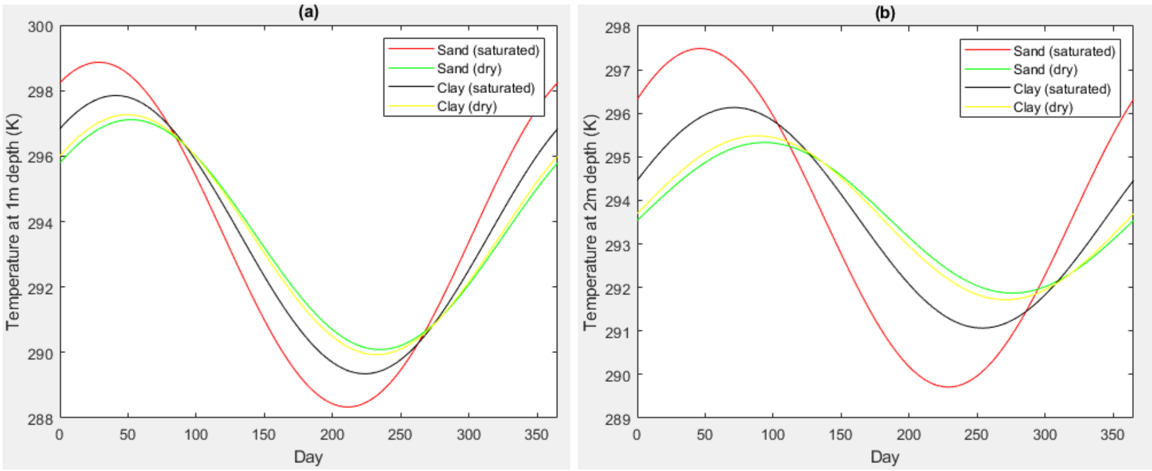

Figure 4. (a): Average temperatures of the soils along the year at 1m depth. (b): average temperatures of the soils along the year at 2m depth

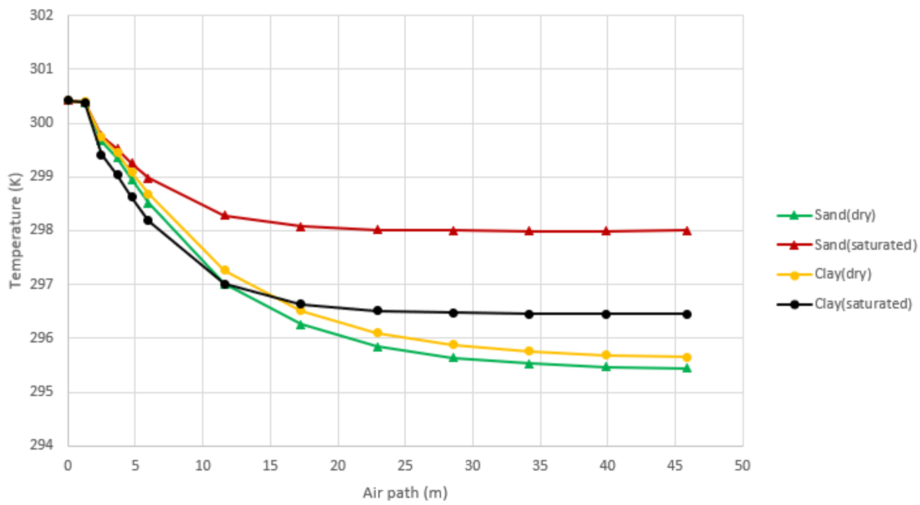

Figure 5. Average temperatures profiles on 01/23/2022.

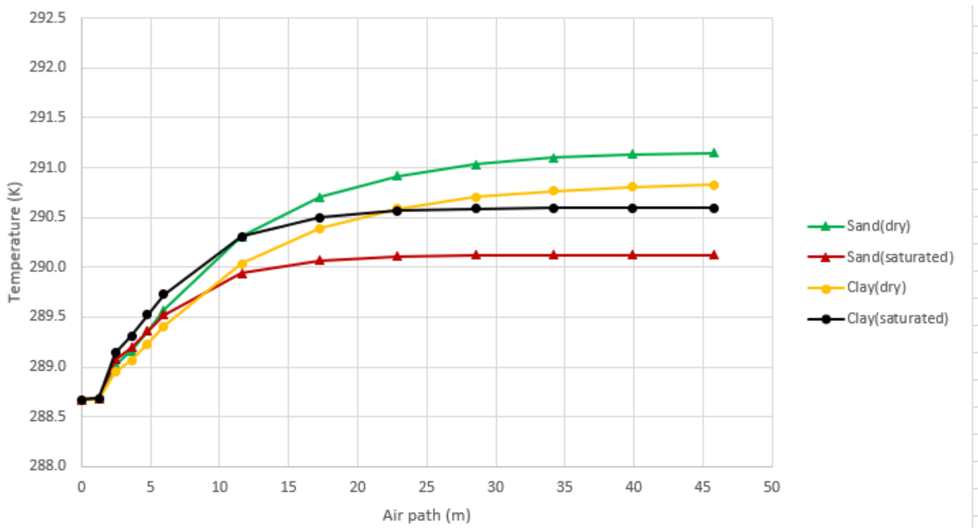

Figure 6. Average temperatures profiles on 08/20/2022.

Table 7 shows the inlet and outlet temperatures for all the soils at 18:00 h on 01/23/2022, which was the time of that day when the inlet temperature reached its highest point. It also displays the inlet and outlet temperatures at 04:00 h on 08/20/2022, which is the time of that day when the inlet temperature reached its lowest point.

Table 7. Inlet and outlet temperatures (K) for each soil at 18:00 h on 01/23/2022 and at 04:00 h on 08/20/2022.

	Sand (dry)	Sand (saturated)	Clay (dry)	Clay (saturated)
01/23 - inlet	302.9	302.9	302.9	302.9
01/23 - outlet	295.5	298.0	295.7	296.5
08/20 - inlet	288.2	288.2	288.2	288.2
08/20 - outlet	291.2	290.1	290.8	290.6

The dry sand performed better in both scenarios, warming up the air during the coldest part of a cold day by 2.9 K and cooling it down during the hottest part of a hot day by 7.5 K. However, the same sand had the worst performance among the analyzed soils when saturated, with a water content of 20.2%, cooling the air at 18:00 h on 01/23/2022 by only 4.9 K and warming it up by 1.9 K at 04:00 h on 08/20/2022. As shown in Fig. 5 and Fig. 6, the average temperatures in each analyzed case indicate that the EAHE performs better when the soil is dry. Compared with the saturated sand, the dry sand had an average outlet temperature of 2.6 K cooler on 01/23/2022 and 1 K warmer on 08/20/2022. In the case of the clay soil, it was observed that on 01/23/2022, the average outlet temperature of the air using dry clay was 0.8 K cooler than when using saturated clay. In contrast, on 08/20/2022, the average outlet temperature of the air using dry clay was 0.2 K warmer than when using saturated clay.

4 Conclusions

In both cases (summer and winter), dry sand and dry clay had the best performances. This fact suggests that dry soils with lower thermal diffusivity are more efficient for the climatic conditions used in the simulations (25.1° South, 50.16° West).

On the contrary, the saturated soils exhibited a greater thermal amplitude throughout the year due to their higher thermal diffusivity compared to the dry soils. As a result of these characteristics, the saturated soils did not perform as well as the dry soils in this context, in which a greater depth for the installation of the exchanger could be indicated. The temperature differences in the air outlet of the EAHE confirm the advantage of the dry soils in terms of thermal exchange performance.

Acknowledgements. This research was supported by the Federal University of Technology - Parana and Brazilian agencies: Coordination for the Improvement of Higher Education Personnel (CAPES) and the Brazilian National Council for Scientific and Technological Development (CNPq).

Authorship statement. The authors hereby confirm that they are the sole liable persons responsible for the authorship of this work, and that all material that has been herein included as part of the present paper is either the property (and authorship) of the authors, or has the permission of the owners to be included here.

References

[1] International Energy Agency (IEA). “The future of cooling: opportunities for energy efficient air conditioning”. Paris, 2018.
[2] M. Khabbaz et al. “Experimental and numerical study of an earth-to-air heat exchanger for buildings air refreshment in Marrakech”. 14th International Conference of the International Building Performance Simulation Association, 2015.
[3] R. S. Brum. Modelagem computacional de trocadores de calor solo-ar. Master’s thesis, UFRGS, 2013.
[4] D. D’Agostino et al. “The Energy Performances of a Ground-to-Air Heat Exchanger: A Comparison Among Köppen Climatic Areas”. Energies, 2020.
[5] R. Misra et al. “CFD analysis based parametric study of derating factor for Earth Air Tunnel Heat Exchanger”. Applied Energy, vol. 103, p. 266-277,2013.
[6] C.H. Diedrich.; G. H. Santos.; G. C. Carraro.; V. V. Dimbarre.; T. A. Alves. “Numerical and Experimental Analysis of an Earth–Air Heat Exchanger”. Atmosphere 2023, 14, 1113.

[7] T. Kusuda. and P.R. Archenbach. "Earth Temperature and Thermal Diffusivity at Selected Stations in the United States", ASHRAE Transactions, Vol. 71, Part 1, 1965.
[8] J. C. Tannehill.; D. A. Anderson.; R. H. Pletcher. *Computational fluid mechanics and heat transfer*. Taylor & Francis, 1997.
[9] C. H. Diedrich.; D. P. Vasconcellos.; V. V. Dimbarre.; G. H. Santos.; T. A. Alves. "Trocador de Calor Solo-Ar (TCSA): Uma Alternativa Sustentável para Condicionamento de Ar". XXII CONEMI, 2021.
[10] I. N. Hamdhan and B. G. Clarke. "Determination of Thermal Conductivity of Coarse and Fine Sand Soils". World Geothermal Congress, 2010.
[11] N. Mendes.; G. H. Santos.; R.Z. Freire.; M.O. Abadie. "Heating and Cooling Potential of Buried Pipes in South Brazil". 11th Brazilian Congress of Thermal Sciences and Engineering, 2006.
[12] L. H. Maia. Comparação Numérica-Experimental do Desempenho Térmico de um Trocador de Calor Solo-Ar. Undergraduate thesis, UTFPR – Ponta Grossa, 2022.
[13] L. C. Victoria.; , I. S. Vaz.; J. Costi.; L. A. O. Rocha.; E. D. Santos; M. K. Rodrigues.; L. A. Isoldi. "Estudo numérico de desempenho de trocadores de calor solo-ar em cidades do Rio Grande do Sul". Ciência e Natura, Santa Maria, v. 43, Ed. Esp. X ERMAC RS, e5, p. 1-12, 2021.